Print-on-Demand Facsimile of Online Articles

PALAIOS

Emphasizing the Impact of Life on Earth's History

September 2014 Volume 29, No. 9

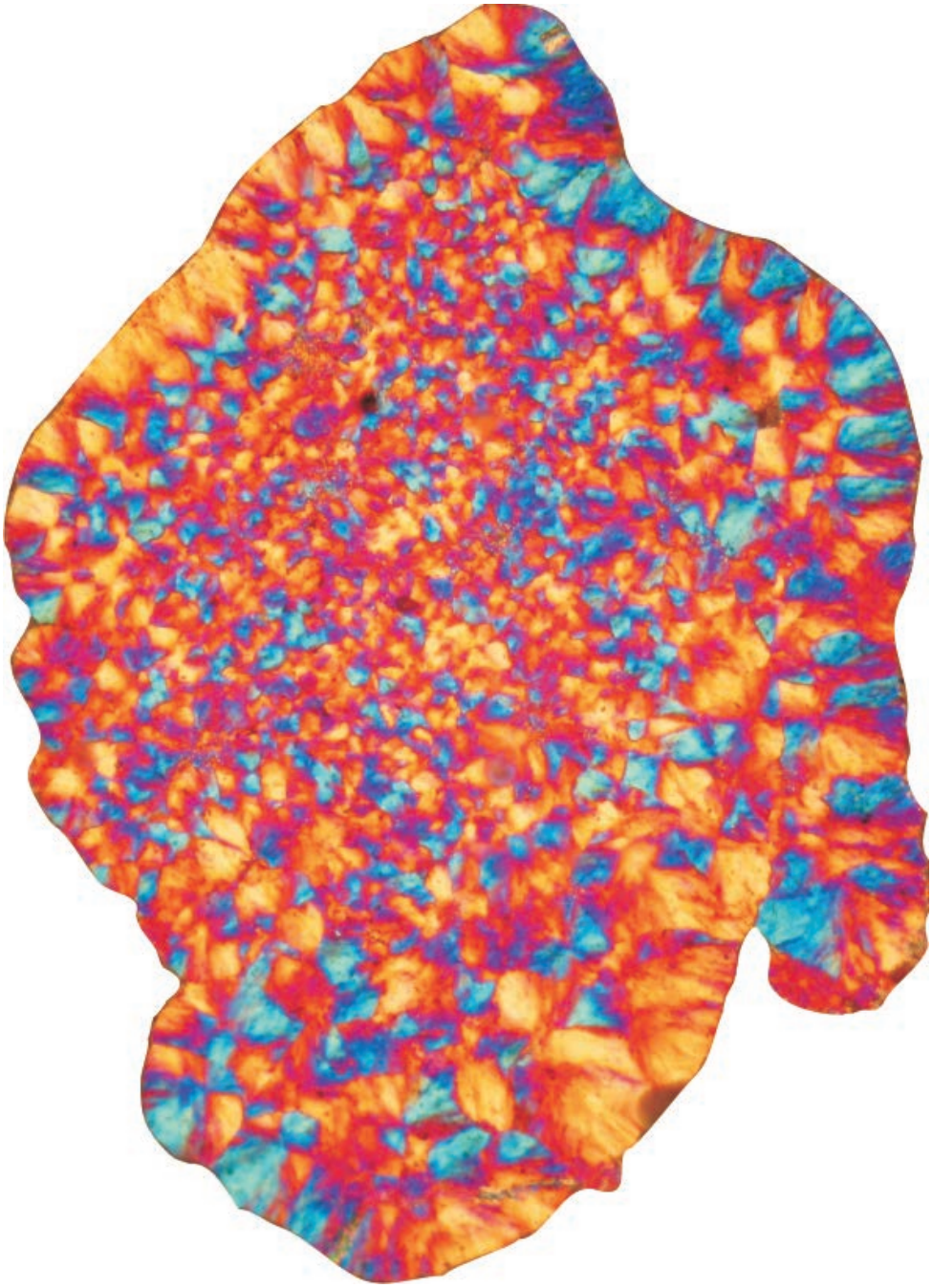

An International Journal of SEPM
(Society for Sedimentary Geology)

PALAIOS
Emphasizing the impact of life on Earth's history

PALAIOS, 2014, v. 29, 449–459
Research Article
DOI: http://dx.doi.org/10.2110/palo.2014.060

CHEMOMETRIC APPROACH TO CHAROPHYTE PRESERVATION (TRIASSIC CERRO PUNTUDO FORMATION, ARGENTINA): PALEOLIMNOLOGIC IMPLICATIONS

CECILIA A. BENAVENTE,[1] JOSÉ A. D'ANGELO,[1,2] ESTEBAN M. CRESPO,[3] AND ADRIANA C. MANCUSO[1]

[1]*Instituto Argentino de Nivología, Glaciología y Ciencias Ambientales (IANIGLA), Centro Científico Tecnológico - Consejo Nacional de Investigaciones Científicas y Técnicas (CCT-CONICET-Mendoza), Avda. Ruiz Leal s/n Parque Gral. San Martín (5500) Mendoza, Argentina*

[2]*Área de Química, Facultad de Ciencias Exactas y Naturales, Universidad Nacional de Cuyo, Mendoza, Argentina*

[3]*Laboratorio de Microscopía Electrónica y Microanálisis (LABMEM), CCT- CONICET, Universidad Nacional de San Luis, Mercedes, San Luis, Argentina*

e-mail: cebenavente@gmail.com

ABSTRACT: A first-time chemometric study of energy-dispersive X-ray (EDX) data of Charophyta gyrogonites is presented. Specimen provenance is a microbialitic carbonate lacustrine succession from the Triassic (Anisian, 243.8 ± 1.9 Ma) of the Cerro Puntudo Formation, San Juan, Argentina. Gyrogonites from three different strata of the succession are studied. Data obtained by EDX include major and minor components, which are analyzed by principal component analysis (PCA). The aim of this study is twofold: first to determine the preservation features of gyrogonites by way of a chemometric approach (i.e., EDX followed by PCA) and then to infer the likely, original chemical composition of the paleolake inhabited by charophytes. EDX spectra show the presence of O, Ca, and minor elements (e.g., Si and Mg), indicating a predominantly calcium carbonate ($CaCO_3$) composition. Principal component analysis supports differences obtained between central and peripheral areas of the gyrogonites, indicating a higher $CaCO_3$ content in their central part. On the other hand, in their outer part, the $CaCO_3$ diminishes and the presence of Si compounds is recorded. No significant differences among gyrogonites from the three different strata are found, implying a similar preservation mode. This suggests a differential diagenetic pattern for the external cells of the gyrogonites than their centers. These results have implications regarding the chemical composition of the paleolake water (Si and Ca availability) and the provenance and catchment areas. Results are encouraging regarding the usefulness of a chemometric approach for studies of fossil remains in lacustrine environments when other techniques of chemical analysis are not available.

INTRODUCTION

Biomineralization is a very common process in different groups of organisms and can take place by different paths (Brasier 1986; Lowenstam and Weiner 1989; Brownlee and Taylor 2002; Weiner and Dove 2003). Differences in the biomineralization process depend on where specifically in the cell precipitation takes place and to what extent it is directly or indirectly regulated by the organisms. The study of mineralization mediated by organisms provides hints about the original chemical composition of their environments and also about biota, since it directly or indirectly determines the variability and diversity of organisms present. This can be applied, with some care, to the chemistry of the paleoenvironments, particularly paleolakes. A similar principle was tested for inferring the chemical composition of waters by analyzing the chemistry of sediments (Krumbein and Garrels 1952). In the case of organisms that biomineralize, the water chemistry can be unraveled from the study of their hard parts (Weiner and Dove 2003; Deocampo 2010). However, when analyzing biomineralization in the fossil record, care must be taken regarding the taphonomy, including both biostratinomy (processes affecting organic remains above the sediment surface) and diagenesis, since these processes can greatly alter and mask original compositions leading to incorrect interpretations (Friedman et al. 1970; Turner et al. 2000). Strong care must be taken because of the numerous factors that can alter the primary composition of the charophytes during taphonomic processes. In the same way as ecologic requirements, the postmortem processes that affect algal remains depend on the chemical composition of the surroundings.

Charophytes are a group of algae that calcify part of their thalli and gyrogonites. Their biocalcification belongs to the extracellular type since it occurs inside the cell wall but outside the cytoplasm where organic matter (OM) acts as nuclei for Ca precipitation, a process named extracytoplasmic calcification (Leitch 1991). The Ca-rich structure that forms is known as calcine and can be distinguished as endo- and ectocalcine according to the stages of calcification (Horn af Rantzien 1956). Endocalcine is the first structure to form and the ectocalcine forms later on. The above-described mechanism has been long known and is a type of biologically induced precipitation (Mann 2001). Despite this, no studies about how the chemical composition of the calcine is affected during taphonomy have been reported. Little is known about how the chemical composition of charophytes is altered after decay, through diagenesis, to its preservation in the sedimentary record.

We present the first chemometric study of selected charophytes belonging to the family Porocharaceae (Benavente et al. 2012a, 2012b). Energy-dispersive X-ray (EDX) analysis followed by evaluation via principal-component analysis (PCA) is employed to determine the preservation characteristics of charophytes and to infer the probable, original chemistry of the paleolake inhabited by these algae. More importantly, our chemometric approach proves to be a reliable analysis tool that could be useful for studying the preservation modes of different paleontological remains when other analytical techniques are not available.

GEOLOGIC SETTING

The studied charophytes were sampled from the Cerro Puntudo Formation which is a microbialitic carbonate lacustrine succession within

Published Online: November 2014
 0883-1351/14/029-449/$03.00

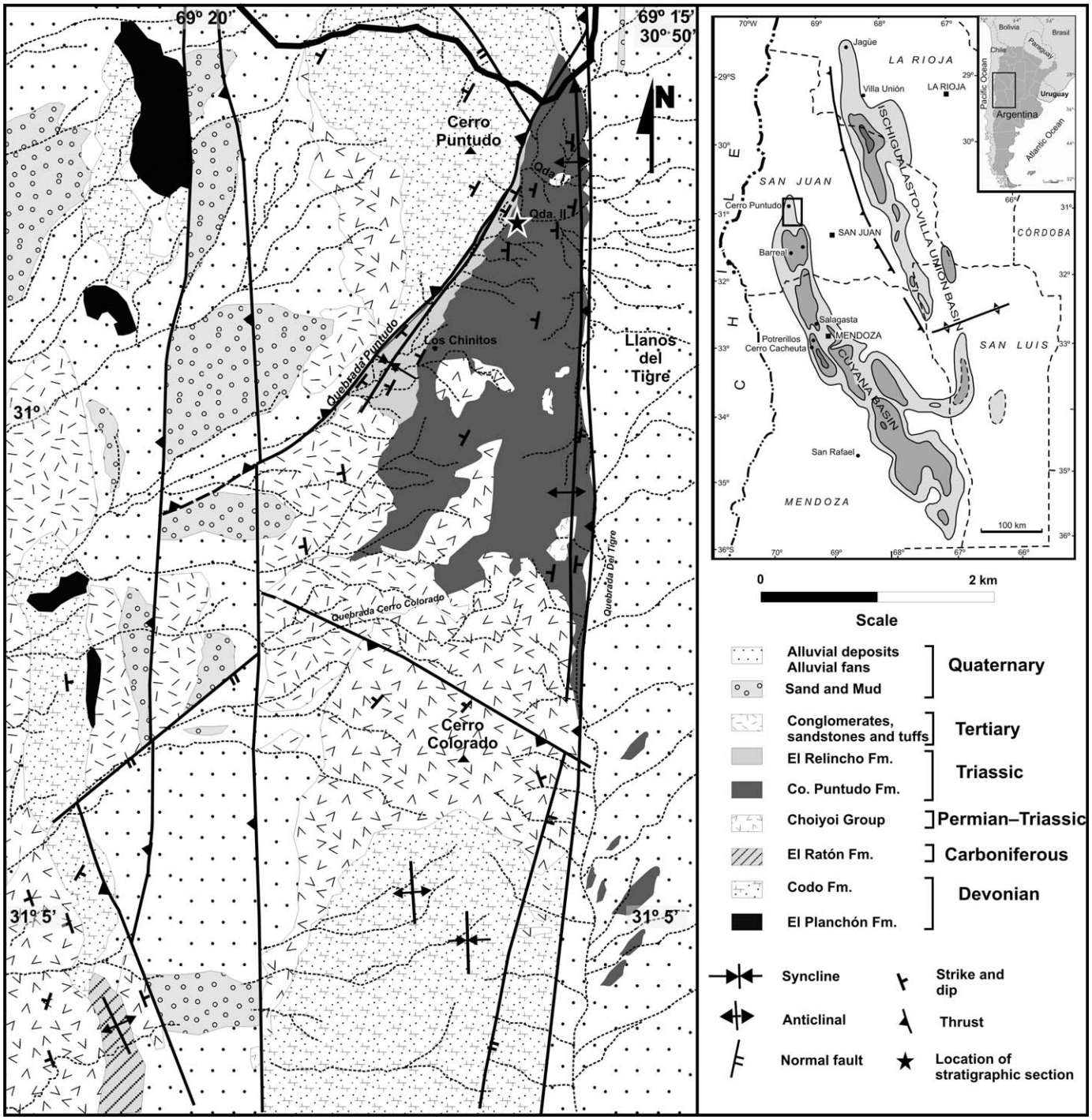

FIG. 1.—Geologic and location map of the Cerro Puntudo subbasin, Cuyana Basin, Argentina.

the Cerro Puntudo subbasin of the Cuyana rift basin. The basin formed as a consequence of the extension that led to the breakup of Pangea along the southwestern margin of Gondwana during the Triassic (Stipanicic 2001), forming half grabens with NNW–SSE orientations (López-Gamundí et al. 1989; Stipanicic 2001). The Cerro Puntudo locality constitutes the northernmost outcrop of the basin located at (30°98′42″S 69°27′42″W) in the Precordillera of San Juan province (Fig. 1).

The Cerro Puntudo Formation has been dated by palynologic and U–Pb zircon (SHRIMP) data as 243.8 ± 1.9 Ma; i.e., Anisian (Mancuso et al. 2010). The formation displays four main facies associations (Fig. 2) that characterize a typical alluvial–lacustrine succession, including a proximal–medial alluvial fan system (CP-A), a fluvial system associated with a distal alluvial fan system (CP-B), a fluvial system interbedded with lacustrine deposits (CP-C), and a lacustrine system (CP-D) (López-Gamundí and Astini 2004; Mancuso et al. 2010). The CP-D facies association consists mainly of alternating biogenic limestones, mudrocks, siltstones, sandstones, and tuffs. The limestones represent pond settings probably fed by Ca-rich springs that developed on an alluvial plain

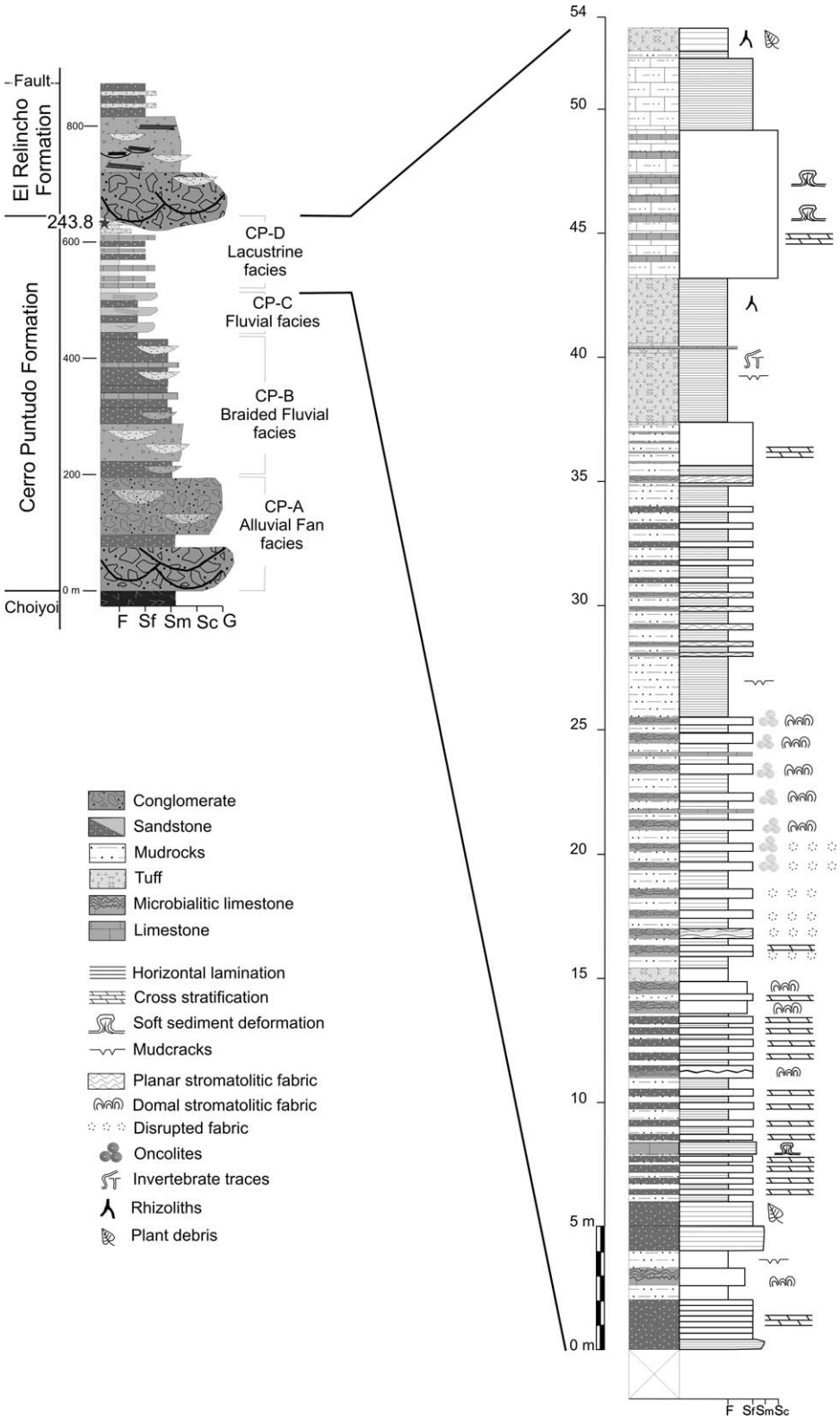

FIG. 2.—General and detailed stratigraphic log of the Cerro Puntudo Formation (Anisian) in the Cerro Puntudo subbasin, Cuyana Basin, Argentina.

(Benavente et al. 2012b). The biogenic limestones of the CP-D facies association include three characteristic facies: (1) stromatolitic limestones (Ls) containing stromatolites *sensu stricto* (planar lamination); (2) disrupted micritic limestones (Lmd) with pedogenic features; and (3) oncolitic limestone (Lo) consisting of microbialites with spherical lamination (Benavente et al. 2012b). The charophytes studied are found as abundant gyrogonites and scarce thalli fragments in the Lo facies. The carbonate beds of the Lo facies are light gray in color and massive with dispersed oncolites and erosive basal contacts (Benavente et al. 2012b). These lenses vary in thickness from 8 to 68 cm (Fig. 2), interbedded with

siliciclastic mudstones of 3 cm up to 1 m in thickness. The provenance of the Cerro Puntudo limestones has been determined by $^{86}Sr/^{87}Sr$ isotopes to be derived from the volcanic deposits of the Permian–Triassic Choiyoi volcanism event (Benavente 2014).

MATERIALS AND METHODS

The charophytes were first observed in thin sections from limestone beds of the CP-D facies association under a petrographic microscope (Olympus BX-51). Thereafter, hand samples from these beds were processed using the copper sulfate method for calcareous microfossil extraction (after Feist et al. 2005) at the Laboratorio de Palinología, of the Instituto Argentino de Nivología, Glaciología y Ciencias Ambientales (IANIGLA) of Mendoza. The gyrogonites, derived from three different beds of the Lo facies, were recovered from rock fragments using needles and a brush under a binocular low-magnification microscope (Nikon NI-150 SMZ 1000). The material is housed at the Museo de Ciencias Naturales y Antropológicas Juan Cornelio Moyano of Mendoza under collection numbers MCNAM-PB 1520, 1521, 1522, and 1523.

The sample designations correspond to the unit names and paleoenvironmental interpretation (CPL stands for Cerro Puntudo Formation, lacustrine) and a correlative number that reflects the limestone unit in the log from which the samples were taken. Association designation corresponds to the unit name (CP = Cerro Puntudo).

Scanning Electron Microscopy and Energy-Dispersive X-Ray Spectrometry

Micrographs were obtained using a scanning electron microscope at the Laboratorio de Microscopía Electrónica y Microanálisis (LabMEM) of the Universidad Nacional de San Luis (UNSL). Spectrochemical data were obtained using scanning electron microscopy (SEM) in combination with energy-dispersive X-ray spectrometry (SEM-EDX). Samples were carbon coated before examination. Chemical compositions were obtained through a scanning electron microscope (JEOL JSM-6610 LV) with an energy-dispersive spectrometer attached (Thermo Scientific Ultra Dry Noran System 7). Elements with atomic number greater than 5 were detected by the Sapphire Ultra-Thin Window X-ray detector, with a resolution of 129.2 eV for the Mn-Kα line. Acquisition time was 100 seconds, nominal incident beam energy (E_o) was 15 keV, and working distance was 15 mm.

EDX measurements were performed in three selected sample areas—i.e., three sample types: (1) gyrogonite central area (C), (2) gyrogonite peripheral area (P), and (3) the rock matrix (M). For comparison purposes, a single $CaCO_3$ sample (high purity, 99.5%) was included as a fourth sample.

EDX measurements have to be performed on well-polished specimens so that surface roughness does not affect the results. However, the particular features of the samples under study do not allow adequate polishing, thus yielding semiquantitative results (see the next section below). The latter have adequate precision required for multivariate statistical analyses.

Point measurements by EDX were used for monitoring trends in elemental distributions (major and minor components). Locations of measurement points were chosen at preset intervals. However, in some instances, point positions were manually modified to an adjacent area in order to avoid rock or fossil pore spaces, thus assuring a sufficiently flat surface area for the electron beam. At each point the weight percent of six elements, (O, Mg, Al, Si, K, and Ca) was obtained. The estimated reproducibility is within 10%.

Semiquantitative Determinations.—Applications of semiquantitative EDX analysis to the study of fossil materials have proven to be very reliable, providing reproducible results (e.g., Klug et al. 2009; Lin and Briggs 2010; Thomas et al. 2012; Previtera et al. 2013). The absolute method used (as opposed to a relative method) does not need standards (e.g., Vázquez et al. 1988, 1990; Barrea and Mainardi 1998; D'Angelo et al. 2002), and the samples provide all the experimental information required, since well-known physical processes are involved. The absolute or standardless analysis is based on the Fundamental Parameters method, where all parameters are derived from theoretical equations, the fundamental parameter database, and precise modeling of the detector, X-ray tube, and geometry. As mentioned above, and because of the sample characteristics, obtaining specimen surfaces smooth enough (the ideal surface being highly polished) for a quantitative analysis is not possible. Inconsistencies in takeoff angles between measured areas and between samples (Goldstein et al. 1992, 2007) are derived from surface roughness that yields semiquantitative results. Thus, semiquantitative elemental concentrations are obtained from measurements of X-ray fluorescence intensities, which are emitted by each element in the specimen.

The characteristic X-ray fluorescence intensity, Ij, emitted by each element in a sample is recorded and then compared with the corresponding intensity I(j) emitted by a standard of concentration C(j). As a first approximation, the intensity Ij may be considered as proportional to the mass concentration Cj of element j:

$$Ij / I(j) = Cj / C(j)$$

Comparisons with the standards allow eliminating physical and geometrical factors, which are very difficult to determine (Goldstein et al. 1992, 2007). Matrix effects must be taken into account using ZAF correction (e.g., Philibert 1963). Z and A factors represent the generation, scattering, and absorption effects, whereas the F factor involves secondary fluorescence enhancement. Since these effects may differ from sample to standard, the ZAF correction is necessary in order to accurately relate the sample composition with the measured, characteristic X-ray fluorescence intensities (Reed 1993). The magnitude of the Z, A, and F correction factors strongly depends on the experimental conditions, mainly on the incident beam energy, X-ray takeoff angle, and differences in composition of the standards used for comparisons. Matrix effects involve all elements in the sample, with a complex functional dependence on the concentrations.

ZAF terms are calculated from suitable, long-accepted, and well-established physical models. Matrix effect corrections are routinely accomplished using the PROZA Phi-Rho-Z matrix correction algorithm (e.g., Bastin et al. 1986; Bastin and Heijligers 1990).

Results from semiquantitative determinations of major and minor components by means of EDX have estimated statistical errors (not shown) in elemental concentrations that can differ by as much as 10% of the values.

Concentration data were transformed to 100%; this treatment admits no incompleteness and avoids the problem of biased correlation coefficients due to the closure effect (see Zodrow 1974).

PCA of EDX-Derived Data: A Multivariate Approach.—Semiquantitative data were analyzed by Principal Component Analysis (PCA). Two components (explained cumulative variance 76.78%) were retained for statistical analysis (Kaiser 1960; see Kendall 1965 for other methods). The aim was to determine dataset groups to evaluate them as a function of EDX-derived data. PCA was performed using STATISTICA® (StatSoft, Inc. 2004) on raw data consisting of the six variables (elements), with 35 determinations each.

RESULTS

Microfacies Features

The microfacies fabric of the Lo facies consisted of coated grains in a matrix composed predominantly of primary micrite and with minor

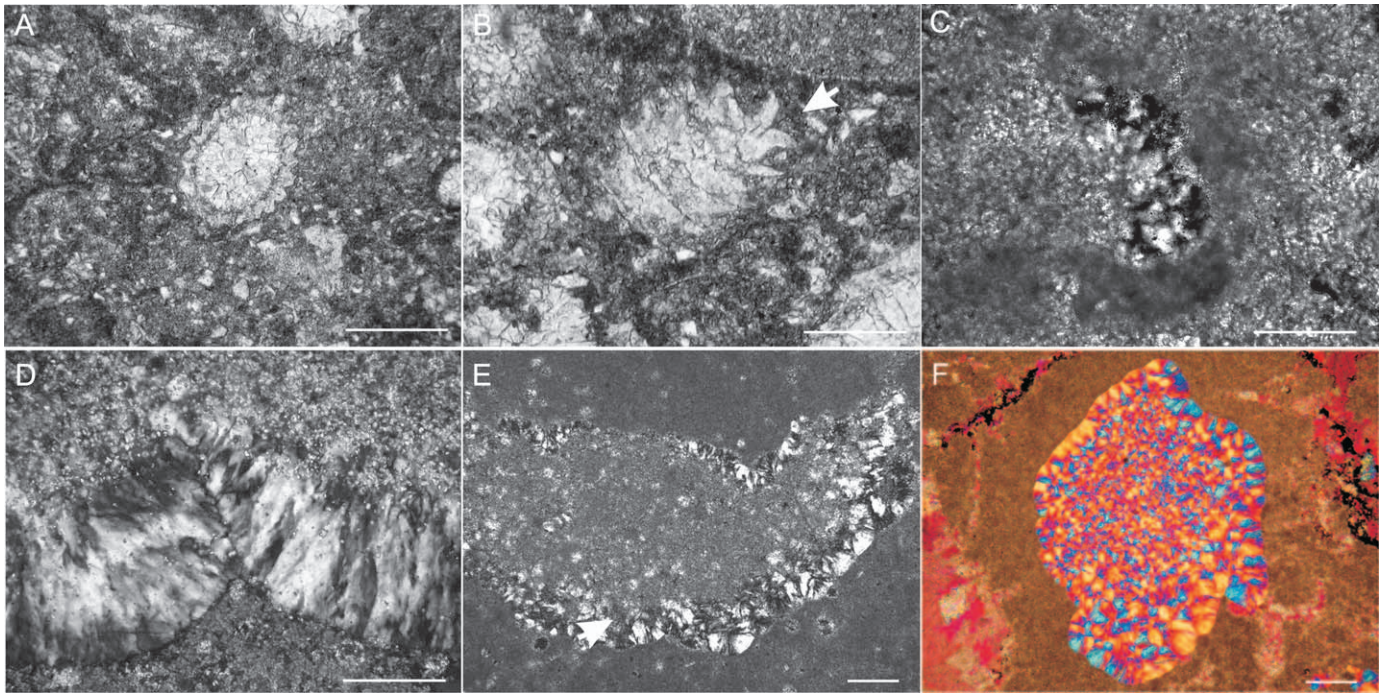

FIG. 3.—Microphotographs of the oncolitic limestone facies (Lo). **A**) Gyrogonite with the apex not ending in a projection, diagnostic of the Porocharoideae subfamily. Scale = 600 µm. **B**) Gyrogonite with a necklike apex (arrow), diagnostic of the Stellatocharoideae subfamily. Scale = 600 µm. **C**) Microcrystalline quartz as equant crystal mosaics. Scale = 150 µm. **D**) Detail of the crystals of zebraic chalcedony. Scale = 100 µm. **E**) Zebraic chalcedony infilling pores, ostracode valves, and fringing microbial micrite (peloidal texture) with micrite inclusions. Scale = 100 µm. **F**) Detail of the length-slow chalcedony observed under the petrographic microscope with a gypsum plate inserted from the southeastern quadrant. Scale = 100 µm.

siliciclastic silt grains. Coated grains were mainly oncolites that varied in size from 0.5–12 cm in diameter with both single and composite forms (Benavente et al. 2012b). They presented a defined nucleus and a cortex with multiple laminae. The nucleus of the oncolites contained Porocharacean gyrogonites that belong to the Stellatocharoideae and Porocharoideae subfamilies (Benavente et al. 2012a, 2012b). The cortex laminae of the oncolites were produced by filamentous algae precipitating Ca during life processes (Benavente et al. 2012b). The occurrence of the algae in the oncolites and the sedimentology of the facies revealed that these filamentous algae were epiphytic and encrusted Charophyta in shallow carbonate ponds. Detached gyrogonites acted as precipitation nuclei allowing oncolite formation (Benavente et al. 2012b). The gyrogonites of both subfamilies consisted of concave calcines that indicated that biomineralization was not strong (Fig. 3A, B). In modern settings, calcine precipitation is controlled mainly by environmental factors like temperature and mineral concentration in the water (Leitch 1991). Other bioclasts, such as ostracode valves and plant remains (stem fragments), were found dispersed in the carbonate matrix as well.

The presence of Si microcrystalline quartz as equant mosaics was common in the Lo facies (Fig. 3C). In addition, length-slow zebraic chalcedony (Fig. 3D, F) was the most abundant crystallization type in the facies, infilling pores and ostracode valves and fringing peloidal microbial micrite (Fig. 3E).

Qualitative EDX Analyses.—Gyrogonite EDX spectra showed high-intensity peaks of O and Ca, indicating a predominantly calcium carbonate ($CaCO_3$) composition (Figs. 4A–D). However, minor elements (i.e., Mg, Al, and Si) were also recorded in some gyrogonite specimens. Rock matrix EDX spectra exhibited O, Mg, Al, and Si peaks, indicating the major components of silicate composition. Smaller peaks of K, Ca, and Fe were present in the rock matrix as well.

PCA of All Sample Types.—The semiquantitative EDX technique provided a large number of data points (210: 35 samples over six attributes; Table 1) which were analyzed using PCA (Fig. 5A, B, see also Supplementary Data). Cumulatively, two components account for 76.78% of the variance. Mainly negative loadings are involved in the first PC (57.81% of variance) with the exception of Ca, which emphasized the relative abundance of Ca compounds (likely $CaCO_3$) versus the other carbonate and silicate minerals (Fig. 5A). The rock matrix sample exhibited the most negative scores (Fig. 5B), indicating the low content of Ca and the importance of compounds containing Si and Al as well as Mg and K. This was clearly shown by the low Ca values and the high values of Si in the rock matrix sample, as shown in Table 1.

Rock matrix, many of the gyrogonite samples, and the almost pure $CaCO_3$ sample scored mostly negative on the second PC (Fig. 5B, 18.97% of explained variance) as a result of the O values being among the highest in the entire sample set (Table 1). A number of gyrogonite areas scored positive on the second component, owing to the high Ca content of these samples.

The plot of scores (Fig. 5B) showed the grouping of data as a function of chemical composition and reflected the nature of the different sample areas. Approximate delimited elliptical zones around the data (Fig. 5B) indicate the groupings of the sample types and do not have any statistical significance. The central and peripheral areas of the gyrogonite, along with the almost pure $CaCO_3$ sample, comprised a tight group.

PCA of Central and Peripheral Areas of the Gyrogonite and $CaCO_3$ Sample.—A second principal components analysis was performed using only the 23 samples from the central and peripheral areas of the gyrogonites and the almost pure CaCO3 sample, restricting these to four attributes: O, Mg, Si, and Ca (Fig. 5C, D). A two-component solution with 77.02% cumulative variance was accepted. The groupings of the

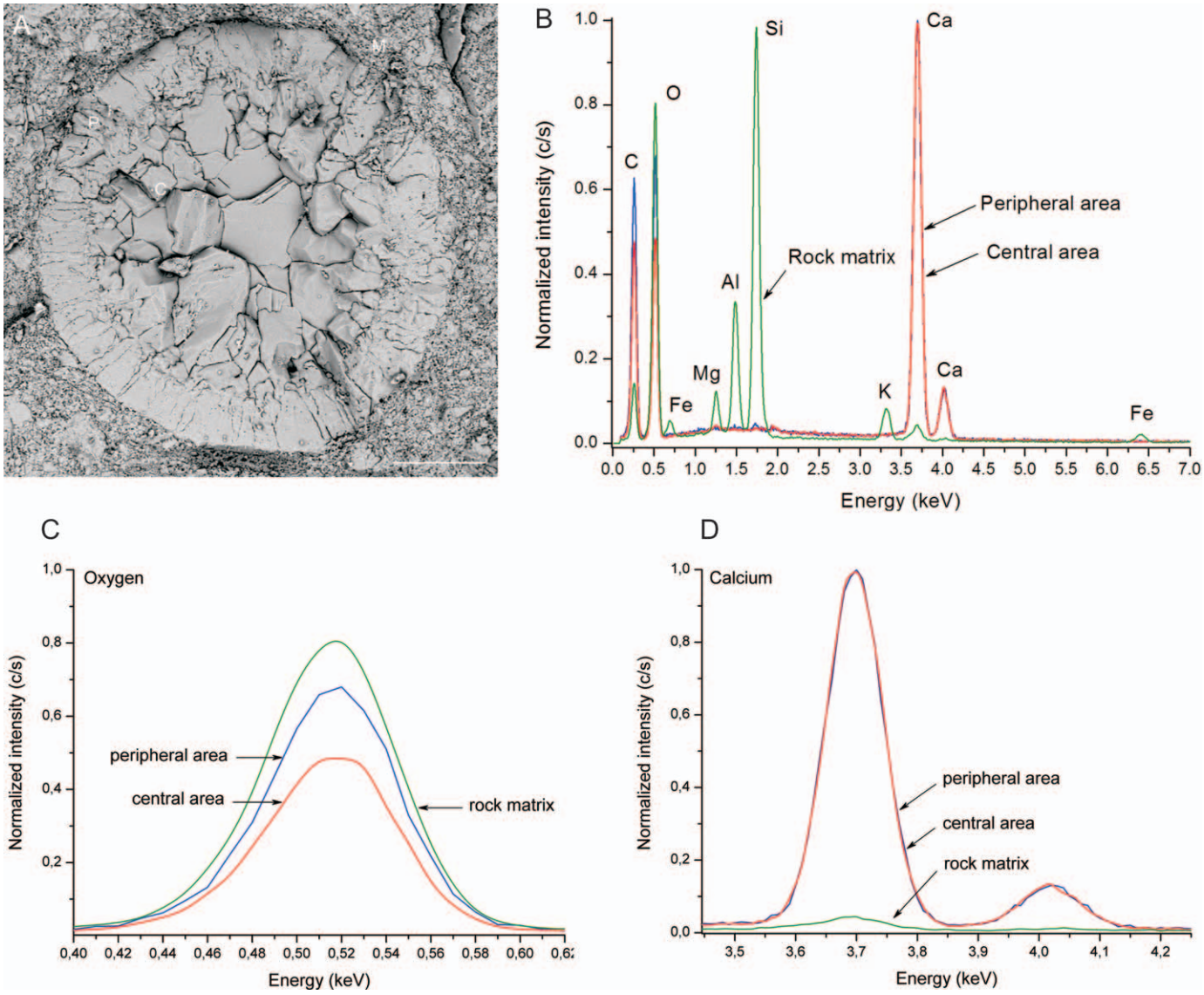

FIG. 4.—Scanning electron microscopy and microanalysis. **A**) Backscatter electron image of a gyrogonite specimen (I 226–CPL 24) showing locations of representative EDX measurement points performed in three selected sample areas: C = gyrogonite central area, P = gyrogonite peripheral area, and R = rock matrix. **B**) Normalized EDX X-ray spectra of rock matrix and representative gyrogonite areas (i.e., center and periphery). **C**) Detail of view B showing oxygen peaks. **D**) Detail of view B showing calcium peaks. See text for further explanation.

different sample types are indicated by delimiting ellipses around the groups for clarity only. The first PC (51.86%) shows a positive loading on O and a negative loading on Ca (Fig. 5C). This component likely reflected the abundance of Ca-containing compounds versus O-bearing (mainly silicate) structures. Most of the central and peripheral areas of gyrogonites exhibited positive scores against the first PC (Fig. 5D) which reflects a higher content of oxygen-containing compounds. $CaCO_3$ is not separable from the central area of gyrogonites (Fig. 5D).

The second PC (25.16% of variance) showed high and intermediate loadings for Mg and Si, respectively (Fig. 5C). Most of the gyrogonite samples and the almost pure $CaCO_3$ sample showed positive scores against the Si component (Fig. 5D), indicating the lower content of silicon-containing compounds.

The plot of scores (Fig. 5D) underlines the useful grouping of data as a function of elemental composition. Gyrogonite areas are illustrated as showing a range of chemical variation. PCA indicates a higher $CaCO_3$ content in the central part of the gyrogonites, while Mg and Si are important components of the peripheral (outer) part.

DISCUSSION

Data Interpretation

The features of Si indicate that its precipitation was part of diagenetic silicification. No amorphous opal (Opal-A) was identified in the microfacies; therefore, it is difficult to link the Si to biogenic precipitation. Also, the development of chalcedony and the absence of other Si crystalline forms (Opal-CT) indicate an advanced silicification process since this form of crystallization usually takes the longest to develop (Bustillo 2010). The chalcedony is length slow, a type that is precipitated in fluids that contain sulfates (SO_4) (Bustillo 2010). Therefore, its presence suggests sulfate-rich fluids circulated through the deposits.

TABLE 1.—*Complete elemental data (O, Mg, Al, Si, K, Ca) of all charophytes, and of the three types analyzed (R = rock matrix, P = peripheral area of the gyrogonite, C = central area of the gyrogonite) from the oncolitic boundstone facies (Lo facies), Cerro Puntudo Formation (Anisian), Cerro Puntudo subbasin, Cuyana Basin. All measurements are expressed as wt%, n.d. = not detected. Sample IDs are reported in Materials and Methods section.*

#	ID	Type	O	Mg	Al	Si	K	Ca
1	I 228 – CPL 22	R	50.62	n.d.	n.d.	2.98	n.d.	46.39
2		R	20.81	0.98	5.25	63.24	4.27	n.d.
3		R	49.83	1.19	5.33	41.87	1.78	n.d.
4		R	49.22	0.58	3.63	44.81	1.02	0.74
5		P	49.26	n.d.	n.d.	0.43	n.d.	50.31
6		P	57.24	n.d.	n.d.	0.34	n.d.	42.41
7		P	35.04	n.d.	n.d.	n.d.	n.d.	64.96
8		P	46.59	n.d.	n.d.	n.d.	n.d.	53.41
9		C	42.81	n.d.	n.d.	n.d.	n.d.	57.19
10		C	53.46	n.d.	n.d.	n.d.	n.d.	46.54
11		C	53.40	n.d.	n.d.	n.d.	n.d.	46.60
12	I 229 – CPL 23	R	47.48	n.d.	1.62	50.6	n.d.	n.d.
13		R	39.69	n.d.	1.10	59.22	n.d.	n.d.
14		R	28.88	n.d.	13.01	51.36	n.d.	n.d.
15		R	42.01	n.d.	0.88	38.35	n.d.	18.76
16		P	52.74	n.d.	n.d.	n.d.	n.d.	47.26
17		P	46.82	n.d.	n.d.	1.57	n.d.	51.61
18		P	40.82	0.42	0.56	0.83	n.d.	57.37
19		P	38.15	0.46	n.d.	n.d.	n.d.	61.39
20		C	43.24	n.d.	n.d.	n.d.	n.d.	56.76
21		C	23.71	n.d.	n.d.	n.d.	n.d.	76.29
22		C	28.96	n.d.	n.d.	n.d.	n.d.	71.04
23		C	53.22	n.d.	n.d.	0.61	n.d.	46.17
24	I 226 – CPL 24	R	48.98	n.d.	1.06	45.08	n.d.	4.88
25		R	38.27	n.d.	n.d.	5.95	n.d.	55.78
26		R	14.14	n.d.	n.d.	8.82	n.d.	77.03
27		R	44.89	3.17	10.16	34.56	4.76	2.47
28		P	52.59	n.d.	n.d.	0.31	n.d.	47.10
29		P	51.93	0.68	n.d.	n.d.	n.d.	47.38
30		P	55.68	0.46	n.d.	0.45	n.d.	43.41
31		P	23.93	n.d.	n.d.	n.d.	n.d.	76.07
32		C	51.01	n.d.	n.d.	n.d.	n.d.	48.99
33		C	47.14	n.d.	n.d.	n.d.	n.d.	52.86
34		C	44.66	n.d.	n.d.	n.d.	n.d.	55.34
35	$CaCO_3$	Pure compound	48.2	n.d.	n.d.	n.d.	n.d.	38.1

Oncolites in modern settings are very common in the discharge aprons of springs (Renaut and Jones 1997; Renaut et al. 1998). Coated grains formed by filamentous algae have been found in hot springs from Iceland (Konhauser et al. 2001). In this type of setting, Si-rich waters are abundant and commonly allow the formation of silicified stromatolites by direct microbial-Si interaction (Konhauser et al. 2001). For the Triassic Lo facies, silicification took place preferentially in the microbialitic matrix, but as a secondary process, not as a biologically induced precipitation.

Paleobiology and Taphonomy

SEM-EDS spectra show the presence of O, Ca, and minor elements like Si and Mg, indicating a predominantly calcium carbonate ($CaCO_3$) composition for the Triassic gyrogonites. The PCA analysis supports differences obtained between central and peripheral areas of the gyrogonites, indicating a higher $CaCO_3$ content in the central part of the gyrogonites. On the other hand, in the outer part of the gyrogonites, the $CaCO_3$ diminishes and Si is present, suggesting a different diagenetic pattern for the external cells of the gyrogonites than their centers. The differences are due to the different chemical compositions of the organisms *in vivo* which also determine the replacement that each part of the structure will undergo during taphonomic processes (Martin 1999). During life, the center of the gyrogonite is composed of the reproductive female cells. After fertilization, extracytoplasmic calcification process of the structure begins, changing the gyrogonite from ectocalcine to endocalcine (Horn af Rantzien 1956).

Biostratinomy.—After death of the algae or detachment of the gyrogonite, the organic matter (OM) decays rapidly in the active taphonomic zone (surface), creating an empty void in the center of the gyrogonite (Fig. 6). In a Ca-rich paleolake, with the appropriate conditions (e.g., pH = 9), calcite will be the first mineral to precipitate, filling the cavity (Siever 1962). This has been observed as spar (calcite cement) in thin section and SEM photographs. At this stage of substrate alteration, the complete structure is calcitic in composition (Fig. 6). For the charophytes that inhabited the Cerro Puntudo paleolake, minimum transport before final burial is proposed. The structures are found in the same setting in which they were formed, and their association with microbial coatings indicates that living charophytes were encrusted by carbonate as a result of epiphytic algal-induced precipitation (Benavente et al. 2012b). In the same way, gyrogonites were also encrusted and when detached from the vegetative thalli became nuclei in the formation of oncolites (Benavente et al. 2012b). Moreover, gyrogonites usually do not undergo much transport in contrast to thalli because they are much heavier (I. Soulié-Marschë, personal communication, 2012). This is in fact reflected in the facies data where gyrogonites are abundant and thalli are scarce. However, when thalli are found, they keep their nodal and internodal sections (Benavente et al. 2012), so transport is considered to be restricted.

The data show that the periphery of the gyrogonites, in all cases, contains Si, and, in two of the three beds analyzed, contains Mg (Table 1). Calcitic charophytes mainly precipitate calcite as low

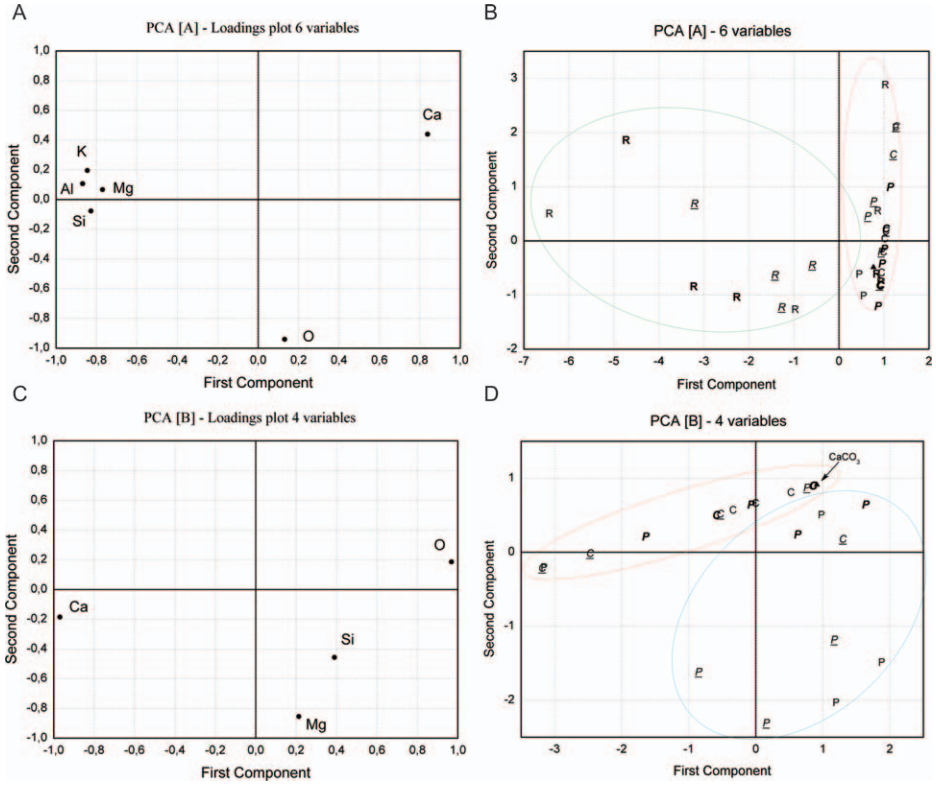

FIG. 5.—Principal component analysis (PCA). **A**) PCA: Plot of component loadings of all data. **B**) PCA: Plot of component scores of all data. **C**) PCA: Plot of component loadings of selected data. **D**) PCA: Plot of component scores of selected data. Approximate delimited elliptical zones are used for clarity only and do not have any statistical significance. In all cases, C = gyrogonite central area measurements, P = gyrogonite peripheral area measurements, and M = rock matrix measurements. See also Supplementary Data.

magnesium calcite (LMC) (Leitch 1991; Martin 1999). The calcine of charophytes that inhabit freshwater settings are strictly LMC while that of brackish water species can be high Mg calcite (HMC) (Feist and Grambast-Fessard 1984). The values found for the periphery of the gyrogonites (Table 1) correspond to the LMC range (0%–5%), indicating that these areas represent part of the original composition and that these charophytes thrived in freshwater paleolakes. Also, the calcification of the calcine can be weak to very strong corresponding to different morphologies (Leicht 1991). Strongly calcified calcines are usually convex and weakly calcified ones are typically concave (Leicht 1991). In this case, gyrogonites are concave (Benavente et al. 2012b) so they were not strongly calcified. Recent work has found that modern charophytes do not calcify when Mg content is high in the water column (Siong and Assaeda 2008). Thus, it can be inferred that the Cerro Puntudo paleolake

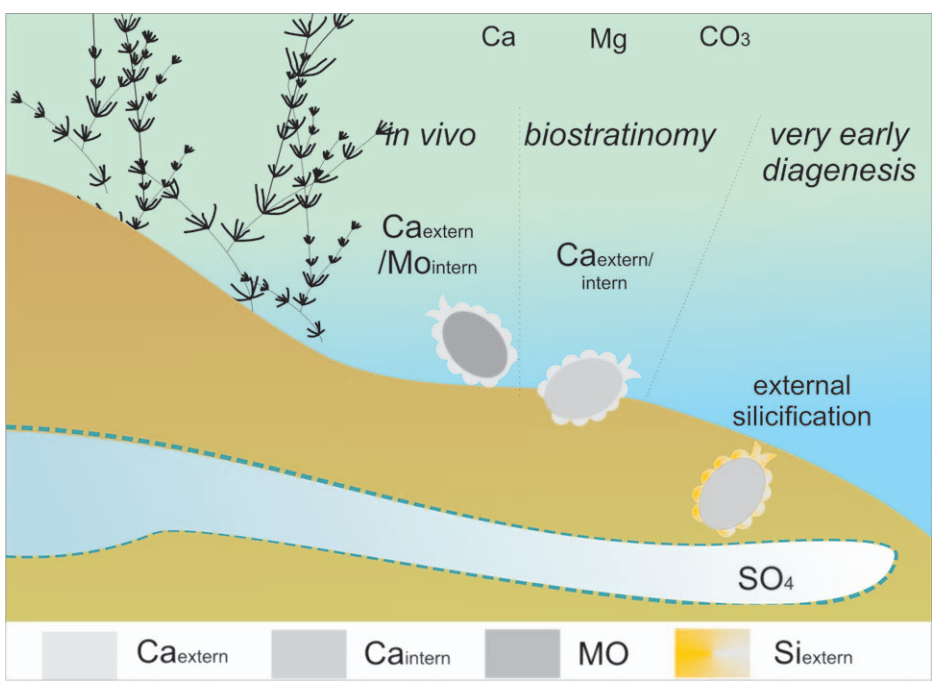

FIG. 6.—Diagram of the inferred taphonomic pathway involved in biomineralization of the charophytes and the processes of very early diagenesis that affected them. Not to scale. *In vivo* stage, the original composition of the gyrogonite is external calcite from the algae biocalcification and internal OM; biostratinomy stage, the external original composition remains but the internal OM has decayed and it has been replaced by secondary calcite; very early diagenetic stage, the external secondary calcite has been replaced by silica and the internal calcite cement remains.

presented a low Mg-Ca ratio, meaning that Mg concentration was in all cases lower than Ca concentration (Table 1) favoring calcification, resulting in concave, weakly calcified (LMC) gyrogonites.

Early Diagenesis.—Regarding the Si content found in the periphery of the gyrogonites, the possibility of contemporaneous Si precipitation has been considered. This process, though very rare, can be triggered by the activity of microorganisms introducing CO_2 into waters and lowering the pH (Knoll 1985). Stromatolites and microbial carbonates can be selectively silicified (De Wet and Hubert 1989; Bustillo et al. 2002). Nevertheless, this mechanism is plausible only in very Si-rich lacustrine environments (Bustillo 2010). Also, in the few cases described, some degradation has been observed suggesting that silicification was indeed part of very early diagenesis (Knoll 1985). Because early diagenetic silicification is a widespread phenomenon in continental carbonates (Knoll 1985; Bustillo 2010) and because of the chalcedony features (zebraic chalcedony), the silicification process of the gyrogonites is interpreted as part of the early burial diagenesis of the Triassic Lo facies.

The diagenetic sequence is as follows: (1) completely calcified gyrogonites are buried. In this stage the external cells of the gyrogonite (periphery) are already biomineralized (LMC original composition). (2) These cells then undergo a secondary replacement, silicification (Fig. 6). In this case, the identification of the textures of the silicate minerals gives information about the time of precipitation and availability in the vadose environment (Bustillo 2010). Carbonate is very reactive, undergoing dissolution and recrystallization in the groundwater-sediment contact zones (Cohen 2003; Bustillo 2010). Therefore it is plausible that Si-rich waters circulating through the deposits during early burial affected the mineral composition of the gyrogonites. Also, silicification is a result of pH and Si concentration equilibrium. For quartz precipitation, for example, the fluid should contain more than 6 mg dm^{-3} and the pH should be less than 7, conditions that also favor calcite dissolution (Bustillo 2010). This situation (lower pH, lower Ca concentration, and soluble silica), in modern playa lake systems, occurs when groundwaters carrying hydrothermal fluids are more dilute due to intermediate or arid local climate conditions (Hardie et al. 1978; Cohen 2003). That relation has been observed in alkaline Lake Bogoria of the East African Rift (Renaut and Tiercelin 1994). A model has been proposed in which the limestone replacement by silica, without development of porosity, occurs if the groundwater is close to equilibrium with respect to calcite (Thiry and Ribet 1999). In the Cerro Puntudo, the chalcedony textures found in the Lo facies correspond to length-slow chalcedony, pointing to the original compositions of the circulating groundwaters as rich in sulfates (Bustillo 2010).

The central zone of the gyrogonites cannot be separated from the almost pure $CaCO_3$ sample, meaning that the chemical (and likely mineralogic) composition is very similar. The central zone most likely reflects the chemical composition resulting from the biostratinomy with the calcite secondary precipitation replacing internal original OM. This calcite cement was not greatly altered by diagenetic processes.

No considerable differences were found among gyrogonites from the three different strata, implying a similar preservation mode. This is consistent with the fact that the limestones are only separated by thin siliciclastic mudstone layers.

Silicon Provenance

Silicification as a process, whether contemporaneous or part of diagenesis, needs a SiO_2 source; possible Si provenance needs to be considered for the Triassic silicified gyrogonites. Silica availability in water in general is highly variable (Brownlee and Taylor 2002). The first source of Si into a lake system is through fluvial input and the second is groundwater input (Hoffman et al. 2002). Moreover, Si is less soluble in superficial waters (Thiry and Ribet 1999), depending on the rocks present in the watershed and the pH of waters (Deocampo 2010).

In the rift setting of the Cerro Puntudo paleolake within the Triassic Cuyana Basin, the main Si source is volcanics, so the Si input would be extraformational (Thiry and Ribet 1999) from the underlying El Choiyoi volcanic complex (Permian–Triassic). The intense volcanic activity of the rifting along with active faulting could have contributed large amounts of Si to the system, especially through the groundwater (Cohen 2003). The Choiyoi Complex developed in the west-central area of Argentina (Spalleti 2001; Kleiman and Japas 2009), covering two stages of volcanism of which the second one ranged from the late Permian to Early Triassic and was acidic (versus the basic first stage) (Llambías and Sato 1989, 1995; Rapalini 1989). Also within the Cerro Puntudo succession, there are numerous and thick tuff interbeds (Fig. 2) (López-Gamundí and Astini 2004; Mancuso et al. 2010) which also could have provided a synsedimentary and intraformational Si volcanic input. In either case, with these rocks in the area, the (perhaps thermal) groundwaters circulating through the Cerro Puntudo paleolake deposits were Si rich. Volcaniclastics are, in general, one of the most important sources for calcium carbonate precipitation (Deocampo 2010). This lithology, by weathering (simple hydrolysis) is one of the most soluble after evaporites (Jones and Deocampo 2005). The Si source and drainage pattern proposed are common in rift basins (Bustillo 2010). Moreover, similar interpretations (Si volcanic source) have been given for lake environments in the Kenya rift of East Africa (Deocampo and Ashley 1999). It has also been observed that Si-rich groundwater can reach wetlands through springs (De Wet and Hubert 1989; Deocampo and Ashley 1999). Recently, the Sr isotopes of the Choiyoi volcanic complex and the Triassic Cerro Puntudo Formation limestones were tested showing that the Sr source probably was the Choiyoi volcanic complex (Benavente 2014).

Silica most likely reached the Cerro Puntudo paleolake through groundwaters in the form of springs (perhaps hydrothermal in nature). In hydrologically closed basins (both surface inflow and outflow), the chemical composition of the lake water depends greatly on the dissolved solutes of the input groundwaters (Hardie et al. 1978; Rosen 1994). Usually in such hydrologically closed scenarios, a saline paleolake tends to develop; composition of brine depends on the rock composition of the drainage (Fig. 7). Only one type of brine could ideally evolve in the Cuyana rift basin, based on the chemistry of the watershed: Ca-Na-Cl brine (Eugster and Hardie 1978; Hardie et al. 1978; Rosen 1994; Jones and Deocampo 2005; Deocampo 2010). This brine type is the result of a hypothetical inflow with Ca > Mg, low SO_4, and low HCO_3, as inferred for the paleolake chemistry for the Triassic Cerro Puntudo deposits (Figs. 5–7). This would explain the weak calcification of gyrogonites and their original LMC composition. This is similar to the chemical composition of groundwater inflow at springs at the East Africa Rift lakes where silica inflow occurs commonly through sublacustrine springs (Renaut et al. 2002, 2012).

CONCLUSIONS

This is the first chemometric study of EDX data of Charophyta gyrogonites preserved in a microbialitic carbonate lacustrine succession from the Triassic (Anisian, 243.8 ± 1.9 my) of the Cerro Puntudo Formation (Cuyana rift basin), San Juan, Argentina. A chemometric approach—i.e., EDX data and subsequent PCA—is used and the following conclusions can be arrived at:

The data provided by the charophytes support the silicification of the gyrogonites during very early diagenesis.

Charophytes of the Cerro Puntudo Formation were exclusively found in the Lo facies. This facies was one of the most common of the carbonates found in the studied succession, and includes microcrystalline

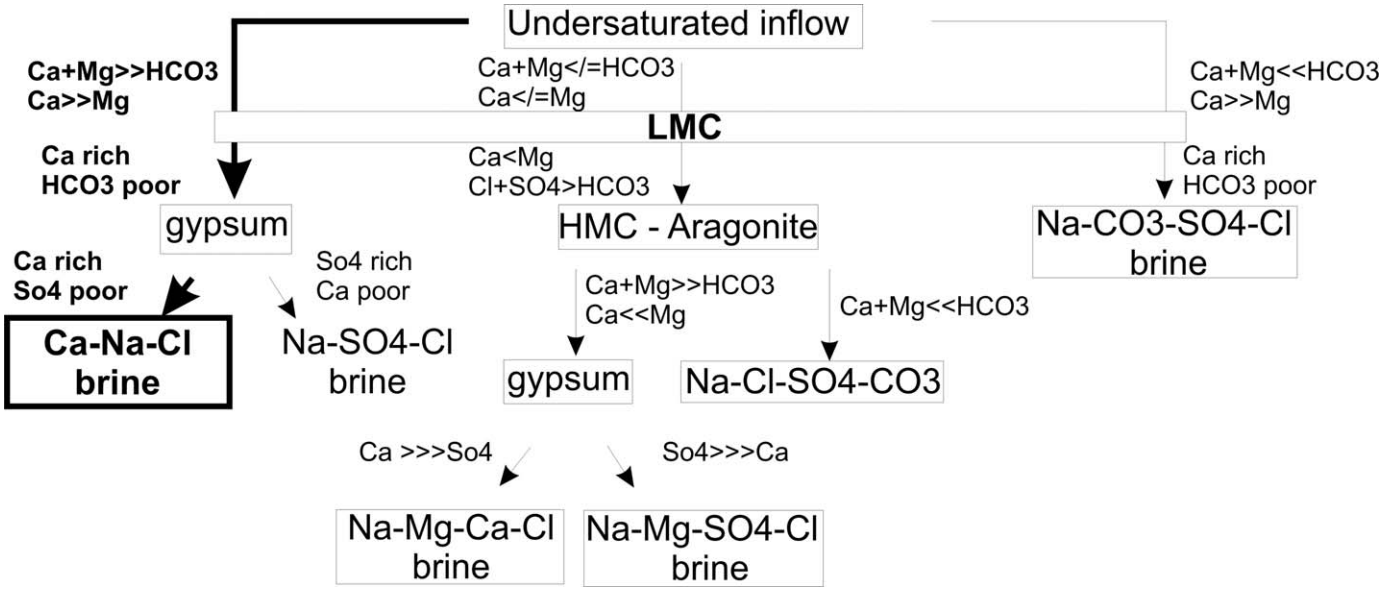

FIG. 7.—Diagram of the possible pathways in an idealized brine evolved from a diluted inflow in a closed lake basin. Modified from Hardie et al. (1978).

quartz and length-slow zebraic chalcedony. This type of silicification is common in diagenetic precipitation, and though it was found fringing microbialites, there was no evidence to suspect organic precipitation. Moreover, analysis revealed that the gyrogonites most likely presented a differential preservation pattern in which the peripheral zone is affected by very early diagenetic silicification and the central zone retains the chemical composition of precipitation during biostratinomy. These chemical differences between the gyrogonite zones and the rock matrix allowed the possible original compositions of the fluids supplied to the paleolake to be inferred. On the one hand, the central zone of the gyrogonites was replaced by spar during biostratinomy, suggesting Ca-rich waters. On the other hand, the peripheral zone of the gyrogonites originally had an LMC composition, but became silicified in minor amounts as part of very early diagenetic silicification processes. The fact that this chalcedony is length slow suggests a sulfate-rich chemical composition of the diagenetic fluids.

The preservation features described above are observed in three different strata in the succession belonging to the Lo facies, which implies a common taphonomic pattern. In addition, during the taphonomic processes affecting charophytes, the external elemental composition resulting from biomineralization of the algae was retained while the internal composition of the gyrogonites underwent secondary precipitation. Therefore, when chemically analyzing and using the structures (gyrogonites) to solve paleoenviromental and paleolimnological issues, the two differential components (peripheral area versus central area of the gyrogonites) must be differentiated . In the rift setting described, the Si-rich groundwaters most likely reached the paleolake as springs at the fault boundaries of the half graben. Regarding the Si provenance, it was probably supplied to the system by weathering of volcanic deposits of the Choiyoi Permian–Triassic volcanism, possibly through groundwater movement.

Results are encouraging regarding the usefulness of our chemometric approach for studies of fossil remains and lacustrine environments when other techniques of chemical analysis are not available.

SUPPLEMENTAL MATERIAL

Data is available from the PALAIOS Data Archive: http://www.sepm.org/pages.aspx?pageid=332.

ACKNOWLEDGMENTS

Authors wish to thank Drs. Elizabeth Gierlowski-Kordesch and Brian Jones for their helpful comments and suggestions that greatly improved the first version of the manuscript. Our thanks are due also to Dr. Thomas Olszewski (Coeditor, PALAIOS), the Associate Editor and the journal reviewers, Prof. E.L. Zodrow (Cape Breton University, Canada), and an anonymous reviewer. They suggested significant changes which improved the quality of presentation and technical contents of the manuscript. Funding for this research was provided by projects PICT 32236 (to ACM), and PIP 11420090100209 (to ACM).

REFERENCES

BARREA, R.A., AND MAINARDI, R.T., 1998, Standardless XRF analysis of stainless-steel samples: X-Ray Spectrometry, v. 27, p. 111–116.

BASTIN, G.F., AND HEIJLIGERS, H.J.M., 1990, Progress in electron-probe microanalysis: Materialwissenschaft und Werkstofftechnik, v. 21, p. 216–221.

BASTIN, G.F., VAN LOO, F.J.J., AND HEIJLIGERS, H.J.M., 1986, Evaluation of the use of Gaussian φ (ρz) curves in quantitative electron probe microanalysis: a new optimization: X-Ray Spectrometry, v. 13, p. 91–97.

BENAVENTE, C.A., 2014, Microbialitas lacustres de secuencias triásicas de Argentina: PhD thesis, Universidad de Buenos Aires, p. 264.

BENAVENTE, C.A., D'ANGELO, J.A., AND CRESPO, E.M., 2012a, Preservation study of Triassic charophytes (Cerro Puntudo San Juan, Argentina). A chemometric approach, *in* A. García, L.D. Rojo, A. R. Chivas, E. J Cáceres, eds., VI International Symposium on Extant and Fossil Charophytes, Mendoza, Argentina, (November 25–27, 2012), Abstracts, p. 21.

BENAVENTE, C.A., MANCUSO, A.C., AND CABALERI, N.G., 2012b, First occurrence of charophyte algae from a Triassic paleolake in Argentina and their paleoenvironmental context: Palaeogeography, Palaeoclimatology, Palaeoecology, v. 363–364, p. 172–183, doi: 10.1016/j.palaeo.2012.09.016.

BRASIER, M., 1986, Why do lower plants and animals biomineralize?: Paleobiology, v. 12, no. 3, p. 241–250.

BROWNLEE, C., AND TAYLOR, A.R., 2002, Algal calcification and silicification: Encyclopedia of Life Sciences, p. 1–6. http://www.mba.ac.uk/fellows/taylor/new_taylor_website/pdfs/Calcification-els.pdf.

BUSTILLO, M.A., 2010, Silicification of continental carbonates, *in* Alonso-Zarza, A.M., and Tanner, L.H., eds., Carbonates in Continental Settings: Geochemistry, Diagenesis and Applications: Developments in Sedimentology, v. 62, p. 153–178.

BUSTILLO, M.A., ARRIBAS, M.E., AND BUSTILLO, M., 2002, Dolomitization and silicification in low energy lacustrine carbonates (Paleogene, Madrid Basin, Spain): Sedimentary Geology, v. 151, p. 107–126.

COHEN, A.S., 2003, Paleolimnology: The History and Evolution of Lake Systems: Oxford, UK, Oxford University Press, 528 p.

D'ANGELO, J.A., PERINO, E., MARCHEVSKY, E., AND RIVEROS, J.A., 2002, Standardless analysis of small amounts of mineral samples by SR-XRF and conventional XRF analyses: X-Ray Spectrometry, v. 31, p. 419–423.

Deocampo, D.M., 2010, Geochemistry of continental carbonates, *in* Alonso-Zarza, A.M., and Tanner, L.H., eds., Carbonates in Continental Settings: Geochemistry, Diagenesis and Applications: Developments in Sedimentology, v. 62, p. 1–59.

Deocampo, D.M., and Ashley, G.M., 1999, Siliceous islands in a carbonate sea: modern and Pleistocene spring-fed wetlands in Ngorongoro crater and Oldupai Gorge, Tanzania: Journal of Sedimentary Research, v. 69, p. 974–979.

De Wet, C.C., and Hubert, J.F., 1989, The Scots Bay Formation, Nova Scotia, a Jurassic carbonate lake with silica-rich hydrothermal springs: Sedimentology, v. 36, p. 857–875.

Eugster, H.P., and Hardie, L.A., 1978, Saline lakes, *in* Lerman, A., ed., Lakes: Chemistry, Geology and Physics: New York, Springer-Verlag, p. 237–293.

Feist, M., and Grambast-Fessard, N., 1984, Plaque basale et phylogénie chez les Charophytes: l'apport des formes jurassiques: Cryptogamie, Algologie, v. 5, p. 112.

Feist, M., Liu, J., and Tafforeau, P., 2005, New insights into Paleozoic charophyte morphology and phylogeny: American Journal of Botany, v. 92, no. 7, p. 1152–1160.

Friedman, G.M., Gebelein, C.D., and Sanders, J.E., 1970, Micritic envelopes of carbonate grains are not exclusively of photosynthetic algal origin: Sedimentology, v. 16, p. 89–96.

Goldstein, J.I., Newbury, D.E., Echlin, P., Joy, D.C., Romig, A.D., Jr., Lyman, C.E., Fiori, C., and Lifshin, E., 1992, Scanning Electron Microscopy and X-ray Microanalysis: A Text for Biologists, Material Scientists, and Geologists. Second edition: New York, Plenum Press, 820 p.

Goldstein, J.I., Newbury, D.E., Joy, D.C., Lyman, C.E., Echlin, P., Lifshin, E., Sawyer, L.C., and Michael, J.R., 2007, Scanning Electron Microscopy and X-ray Microanalysis. Third edition: New York, Springer, 586 p.

Hardie, L.A., Smoot, J.P., and Eugster, H.P., 1978, Saline lakes and their deposits: a sedimentological approach, *in* Matter, A., and Tucker, M.E., eds., Modern and Ancient Lake Sediments: Special Publications of the International Association of Sedimentologists, v. 2, p. 7–41.

Hoffman, A., Roussy, D., and Filella, M., 2002, Dissolved silica budget in the North basin of Lake Lugano: Chemical Geology, v. 182, p. 35–55.

Horn AF Rantzien, H., 1956, Middle Triassic Charophyta of south Sweden: Opera Botanica, v. 1, p. 1–83.

Jones, B.F. and Deocampo, D.M., 2005, Geochemistry of saline lakes, *in* Drever, J.I., ed., Surface and Ground Water, Weathering, and Soils. Treatise on Geochemisty: Amsterdam, Elsevier, v. 5, p. 393–424.

Kaiser, H.F., 1960, The application of electronic computers to factor analysis: Educational and Psychological Measurement, v. 20, p. 141–151.

Kendall, M.G., 1965, A Course in Multivariate Analysis. Third impression: London, Charles Griffin and C. Ltd., 185 p.

Kleiman, L.E., and Japas, M.S., 2009, The Choiyoi volcanic province at 34°S–36°S (San Rafael, Mendoza, Argentina): implications for the late Palaeozoic evolution of the southwestern margin of Gondwana: Tectonophysics, v. 473, p. 283–299.

Klug, C., Schulz, H., and De Baets, K., 2009, Red Devonian trilobites with green eyes from Morocco and the silicification of the trilobite exoskeleton: Acta Palaeontologica Polonica, v. 54, no. 1, p. 117–123.

Knoll, A.H., 1985, Exceptional preservation of photosynthetic organisms in silicified carbonates and silicified peats: Royal Society, London, Philosophical Transactions, v. B311, p. 111–122.

Konhauser, K.O., Phoenix, V.R., Bottrell, S.H., Adams, D.G., and Head, I.M., 2001, Microbial-silica interactions in Icelandic hot spring sinter: possible analogues for some Precambrian siliceous stromatolites: Sedimentology, v. 48, p. 415–433.

Krumbein, W.C., and Garrels, R.M., 1952, Origin and classification of chemical sediments in terms of pH and oxidation–reduction potentials: Journal of Geology, v. 60, p. 1–33.

Leitch, A.R., 1991, Calcification of the charophyte oosporangium, *in* Riding, R., ed., Calcareous Algae and Stromatolites: Berlin Heidelberg, Springer-Verlag, p. 204–216.

Lin, J.P., and Briggs, D.E.G., 2010, Burgess shale-type preservation: a comparison of naraoiids (Arthropoda) from three Cambrian localities: PALAIOS, v. 25, p. 463–467.

Llambías, E.J., and Sato, A.M., 1989, Relaciones geológicas del batolito de Colangüil: Reunión de Geotransectas de América del Sur, Montevideo: Actas, p. 83–87.

Llambías, E.J., and Sato, A.M., 1995, Tectónica y magmatismo en el límite permo–triásico de la Cordillera Frontal: Segunda Reunión del Triásico del Cono Sur, Bahía Blanca: Actas, p. 22–26.

López-Gamundí, O.R., and Astini, R., 2004, Alluvial fan lacustrine association in the fault tip end of a half-graben, northern Triassic Cuyo Basin, western Argentina: Journal of South American Earth Sciences, v. 17, p. 253–265.

López Gamundí, O.R., Alvarez, L., Andreis, R., Bossi, G., Espejo, I., Fernandez-Seveso, F., Legarreta, L., Kokogian, D., Limarino, O., and Sesarego, H., 1989, Cuencas intermontanas, *in* Chebli, G., and Spalletti, L., eds., Cuencas Sedimentarias Argentinas, Serie Correlación Geológica No. 6: Instituto Superior de Correlación Geológica, Universidad Nacional de Tucumán, p. 123–167.

Lowenstam, H.A., and Weiner, S., 1989, On Biomineralization: New York, Oxford University Press, 309 p.

Mancuso, A.C., Chemale, F., Barredo, S., Ávila, J.N., Ottone, E.G., and Marsicano, C., 2010, Age constraints for the northernmost outcrops of the Triassic Cuyana Basin, Argentina: Journal of South American Earth Sciences, v. 30, p. 97–103.

Mann, S., 2001, Biomineralization: Principles and Concepts in Bioinorganic Materials Chemistry: New York, Oxford University Press, 193 p.

Martin, R.E., 1999, Taphonomy. A Process Approach: Cambridge, Cambridge University Press, 508 p.

Philibert, J., 1963, A method for calculating the absorption correction in electronprobe microanalysis, *in:* H. H. Pattee, V. E. Cosslett, A. Engström, eds., Proceedings 3rd International Conference on X-ray Optics and X-ray Microanalysis, Stanford: New York, Academic Press, p. 379–392.

Previtera, E., D'Angelo, J.A., and Mancuso, A.C., 2013, Preliminary chemometric study of bone diagenesis in early Triassic cynodonts from Mendoza, Argentina: Ameghiniana, v. 50, p. 460–468.

Rapalini, A.E., 1989, Estudio paleomagnético del vulcanismo permotriásico de la región andina de la República Argentina: Doctoral thesis, Facultad de Ciencias Exactas y Naturales, Universidad de Buenos Aires, 278 p.

Reed, S., 1993, Electron Probe Microanalysis. 2nd edition: Cambridge, UK, Cambridge University Press, 326 p.

Renaut, R.W., and Jones, B., 1997, Controls on aragonite and calcite precipitation in hot spring travertines at Chemurkeu, Lake Bogoria, Kenya: Canadian Journal of Earth Sciences, v. 34, p. 801–818.

Renaut, R.W., and Tiercelin, J.J., 1994, Lake Bogoria, Kenya Rift Valley-A sedimentological overview *in* eds., Renaut R.W. Last W.M. Sedimentology and Geochemistry of Modern and Ancient Saline Lakes, SEPM Spec. Pub., 50, 101–123.

Renaut, R.W., Jones, B., and Tiercelin, J.J., 1998, Rapid in situ silicification of microbes at Loburu hot springs, Lake Bogoria, Kenya Rift Valley: Sedimentology, v. 45, p. 1083–1103.

Renaut, R.W., Jones, B., Tiercelin, J.J., and Tarits, C., 2002, Sublacustrine precipitation of hydrothermal silica in rift lakes: evidence from Baringo, central Kenya Rift Valley: Sedimentary Geology, v. 148, p. 235–257.

Renaut, R.W., Owen, R.B., Jones, B., Tiercelin, J.J., Tarits, C., Ego, J.K., and Konhauser, K.O., 2012, Impact of lake-level changes on the formation of thermogene travertine in continental rifts: evidence from Lake Bogoria, Kenya Rift Valley: Sedimentology, doi: 10.1111/j.1365-3091.2012.01347.x.

Rosen, M.R., 1994, The importance of groundwater in playas: a review of playa classifications and the sedimentology and hydrology of playas: Geological Society of America, Special Paper, v. 289, p. 1–18.

Siever, R., 1962, Silica solubility 0–200°C and the diagenesis of siliceous sediments: Journal of Geology, v. 70, p. 127–150.

Siong, K., and Assaeda, T., 2008, Effect of magnesium on charophytes calcification: implications for phosphorus speciation stored in plant biomass and sediment of Myall Lake, NSW Australia, *in* Sengupta, M., and Dalwani, R., eds., Proceedings of the 12th World Lake Conference, p. 264–274.

Spalletti, L.A., 2001, Evolución de las cuencas sedimentarias *in* eds., Artabe, A.E. Morel E.M., Zamuner A.B. El Sistema Triásico en la Argentina, pp. 81–101. Fundación Museo de La Plata "Francisco Pascasio Moreno", La Plata.

Statsoft. Statistica - Data analysis software system, version 11, 2012, <http://www.statsoft.com>. Accessed on: Sept. 15th, 2012.STIPANICIC, P.N., 2001, Antecedentes geológicos y paleontológicos, *in* Artabe, A., Morel, E., and Zamuner, A., eds., El Sistema Triásico en la Argentina: La Plata, Fundación Museo de La Plata "Francisco Pascasio Moreno", p. 1–21.

Thiry, M., and Ribet, I., 1999, Groundwater silicification in Paris basin limestones: fabrics, mechanisms, and modeling: Journal of Sedimentary Research, v. 69, p. 171–183.

Thomas, D.B., Chinsamy, A., Conrad, N.J., and Kandel, A.W., 2012, Chemical investigation of mineralization categories used to asses taphonomy: Palaeogeography, Palaeoclimatology, Palaeoecology, v. 316–362, p. 104–110.

Turner, E., James, N.P., and Narbonne, G.M., 2000, Taphonomic control on microstructure in early Neoproterozoic reefal stromatolites and thrombolites: PALAIOS, v. 15, p. 87–111.

Vázquez C, De Leyt, D.V., and Riveros, J.A., 1988, Absolute method for determination of metallic film thickness by X-ray fluorescence: X-Ray Spectrometry, v. 17, p. 43–46.

Vázquez, C., De Leyt, D.V., and Riveros, J.A., 1990, Absolute X-ray fluorescence method for the determination of metal thicknesses by intensity ratio measurements: X-Ray Spectrometry, v. 19, p. 93–96.

Weiner, S., and Dove, P.M., 2003, An overview of biomineralization processes and the problem of the vital effect, *in* Dove, P.M., De Yoreo, J.J., and Weiner, S., eds., Biomineralization: Reviews in Mineralogy and Geochemistry: Washington, DC, Mineralogical Society of America, Geochemical Society, v. 54, p. 1–30.

Zodrow, E.L., 1974, Note on closure correlation: Canadian Journal of Earth Sciences, v. 11, p. 1616–1619.

Zodrow, E.L., 1976, Minres factor analysis of hypersthene data, Strathcona Mine (Ontario, Canada): Mathematical Geology, v. 8, p. 395–412.

Received 11 July 2014; accepted 3 September 2014.